Arabian Journal for Science and Engineering (2022) 47:3089–3104
https://doi.org/10.1007/s13369-021-06045-0

RESEARCH ARTICLE-ELECTRICAL ENGINEERING

Effective PV Parameter Estimation Algorithm Based on Marine Predators Optimizer Considering Normal and Low Radiation Operating Conditions

Ahmed Saeed Abdelrazek Bayoumi[1] · Ragab A. El-Sehiemy[2] · Amlak Abaza[2]

Received: 12 November 2020 / Accepted: 30 July 2021 / Published online: 20 August 2021

Abstract
This paper proposes the Marine Predators Algorithm (MPA) as a new bio-inspired optimization algorithm to extract the parameters of three-photo voltaic models of solar cells. These models are three diode model (TDM), double diode model (DDM) and one-diode model (SDM). The MPA is dependent on the manner of a population of Marine Predators. This optimal strategy allows prey to use an optimal foraging strategy and allows predators to use an intelligent rate policy for encounters. The proposed MPA-based parameter estimation algorithm is tested at normal and low radiation operating conditions. The normal operating condition is employed with the 57 mm diameter commercial silicon solar cell (Case 1), while the Case 2 is based on a multi-crystalline silicon solar cell of area 7.7 cm^2 from Q6-1380 under low irradiance levels. The capability of MPA is validated for the three models compared with other competitive algorithms. Simulation results show that high closeness between the estimated and experimental records reflects the high capability of the MPA with more accurate parameters. The RMSE of 8.43854E−4, 7.59E−4 and 7.561E−4 are achieved for Case 1 by using SDM, DDM and TDM, respectively. While, the RMSE has the best levels of 1.61E−5, 1.46E−5, and 1.42E−5 in Case 2, respectively. Also, the MPA has competitive results compared with several optimization algorithms in the literature as sine cosine, particle swarm, salp swarm, grey wolf optimization algorithms. The proposed MPA has good convergence and robust statistical analysis for different operating conditions of low and high irradiance.

Keywords Marine predators optimization algorithm · PV parameter estimation · PV-electrical models · Multi-crystalline solar cell low radiation solar cells

1 Introduction

The expanding and fluctuations in the prices of the fossil fuels as well as the pollution and solid wastes make the renewable energy sources the best solution to support energy in continues manner and almost no pollution. Solar energy is one promising of renewable energy source because of its widespread over world, little maintenance, noise free and almost conventional fabrication techniques. It is important to find the most accurate model for representing the solar cells/modules for techno-economic benefits in the electrical grids. Many researchers are developed several models as the modeling of solar cell has attracted interest from them to describe its behavior at different environmental conditions as in Refs. [1–6] and for enhancing power performance issue [7–9]. In the previous modeling works, the (*I*–*V*), current versus voltage, characteristic curve is the most important behavior to be formulated. To achieve this target, various developed models describe the characteristic of solar cell systems. The first model is called single-diode model (SDM). The SDM combines between the simplicity and accuracy, as it has only five parameters, hence it is considered the most commonly used in many power applications as in [9–11]. The second model is called second diode model which is abbreviated as DDM. The DDM has seven parameters, with two extra parameters that model the extra added diode compared with SDM, which make the calculations more complicate, but

✉ Ahmed Saeed Abdelrazek Bayoumi
ahmed.bayoumi@eng.kfs.edu.eg

[1] Physics and Engineering Mathematics Department, Faculty of Engineering, Kafrelsheikh University, Kafrelsheikh, Egypt

[2] Electrical Engineering Department, Kafrelshiekh University, Kafrelsheikh 33511, Egypt

it is more accurate. The third presented model is called the triple diode model with abbreviation of TDM. The TDM which is the most complicated of these three models, but it is the most accurate especially in case of low radiation [12–16]. Also modified triple diode versus modified diode models were assessed recently in [17]. From the previous presentation, there are many efforts for modeling solar cell/modules at different environmental conditions of temperature and irradiance.

From the point of applications and real markets, Refs. [18–22] cover the energy hub applications and market requirements with the existence of uncertainty impacts of renewable energy resources. Finding the accurate modeling way is an important issue in energy market and energy hubs. The main merits of the parameter estimation play an important role in power system operation. For controlling the frequency in multi-area system, the parameter of solar cell is modeled by SDM as in [23]. Also, it helps in the operation enhancement of pumping system with synchronous machines as in [24] with using of the third generation of solar cell.

In the viewpoint of solution methodology, several reported methods have been explored in the literature to determine the PV parameters. Most of those methods can be varied between three popular classes. The analytical methods belong to the first one [25–28], which provide formulations for the parameters of the data sheet information or *I–V* characteristic curve data. The metaheuristic methods belong to the second one [29, 30], which describe the problem of the estimation of the PV cell model parameter as an optimization problem. The resulting optimization problem can be solved by metaheuristic optimization techniques. The third one is hybrid approaches based on metaheuristic and analytical techniques, that means some of the parameters are calculated by a metaheuristic optimization algorithm and the remaining set of model parameters are found by analytical approach [31].

The determination of parameters accurately is very important in PV design, optimization, simulations, control and performance evaluation. Therefore, the process and technique of parameters estimation are very necessity. There is continuous development in methods to reach more accurate parameters for engineering problems, this aspect motivates this work to find higher accurate optimization algorithm to emulate the PV model. Table 1 represents the recent metaheuristic approaches used for the parameter estimation of PV cell/ modules As shown above, continuous development of optimization algorithms encourages many researchers in variant engineering fields to utilize and achieve the elevated merits to their own situations.

The MPA is one of these recent techniques. It is nature-inspired optimization algorithm based on the optimal foraging strategy and allows predators to use an intelligent rate policy for encounters. It has been proposed in 2020 [53]. It depends on the behavior of a population of Marine Predators. The Marine Predators's social organization and behavior depend on swarm intelligence and evolutionary heuristic. MPA depends on the prey-predator speed ratio. Brownian motion and levy flight are considered to simulate prey and predator movement. Marine predators rely on their spatial memories and advanced cognitive skills in many activities, such as retrieving food and remembering the places where their food is often obtained.

Through this paper, MPA-based algorithm is developed to achieve the optimal parameters of PV models. However, the main contributions of this paper could be summarized in the following points:

- Develop an efficient MPA-based parameter estimation algorithm for solving three different models of PV cells;
- The proposed MPA-based algorithm is applied at normal and low radiations operating conditions of PV cell;
- The normal operating condition is employed with the 57 mm diameter commercial (R.T.C. France) silicon solar cell, while the second operating case is emulated with the MCSSC of area 7.7 cm^2 from Q6-1380 irradiated by low levels.
- The results obtained from MPA are compared with those obtained by other well-known methods in the literature;
- The proposed MPA-based algorithm is characterized by its high robustness and good convergence rates;
- The estimated performance characteristics for *I–V* and *P–V* of the tested cells are very close to experimental data.

The rest of this manuscript has been formed as: Sect. 2 illustrates the various PV models. The problem formulation is declared in Sect. 3. Section 4 explains the MPA algorithm. Section 5 describes results and discussion. Finally, Sect. 6 concludes the paper findings.

2 Photovoltaic Models

Various models have been used to characterize the physics of PV modules. Practically, the most popular models are single- double- and three-diode models that are abbreviated as SDM, DDM and TDM, respectively. The following subsections present the details of the variant models of PV cells.

2.1 Single Diode Model

The first PV model is the single-diode model (SDM). Figure 1 describes the equivalent circuit of SDM. This model simply consists of a current source IPV in parallel with a diode, resistance (RP) which considers the leakage current

Table 1 Reveiw on meta-heuristic methods applied for parameter estimation problem

Reference #	Comment
[1]	In this study, the extracted of solar cell/modules parameters was employed by using penalty-based differential evolution
[2]	The neural network with radial basis function was developed to identify the electrical models parameters of a photovoltaic module
[3]	An iterative numerical cluster analysis method was developed in this study to extract the parameters of DDM of photovoltaic module parameters
[6]	The Interior branch bound optimization algorithm was extracted for three-diode PV models
[9]	In this study, the third generation of solar cells is modeled by SDM model and investigated for water pumping system. The parameters are extracted by using elephant herd optimization algorithm
[17]	In this study, two soft parameter estimation methods called closed loop particle swarm and elephant herd optimizers were developed for parameter estimation of multi-crystal solar cell. Two models are considered
[29]	The Pattern Search technique was employed on the basis of the experimental data presented in [32] to estimate the parameters of SDM and DDM
[30]	Two PV models for cell and modules, called single diode, double diode, and photovoltaic module, are used in this using Simulated Annealing Approach (SAA)
[33]	This study developed the Moth-Flame Optimization Algorithm (MFO) to extract the modified TDM parameters of the discussed MSC
[34]	The Bacterial Foraging (BF) algorithm was applied for shading and normal conditions
[35]	The GOTLBO method that so-called Generalized Oppositional Teaching Learning Based Optimization aims to enhance the quality and speed of convergence process
[36, 37]	Two hybrid differential evolution methods were proposed for the estimation process and are characterized with good performance in CPU-execution time and accuracy
[38]	The PV model is considered at low solar irradiance levels the Flower Pollination algorithm was developed to estimate its parameters
[39]	Mutative-scale Parallel Chaos Optimization algorithm was proposed for different solar cell models are extracted, i.e., double diode, single diode models for PV module
[40]	Feature detection of solar cells was employed by using the Artificial Bee Colony algorithm
[41]	An optimization method was proposed for parameter identification based on the single and double diode models for a 57 mm diameter commercial (R.T.C. France) silicon solar cell. This method is called as Artificial Bee Swarm Optimization algorithm
[42]	The Harmony Search based algorithm (HS) was proposed for identifying the parameters of the solar cell single and double diode models
[43]	The Genetic algorithm was proposed to obtain the global optimal parameters for SDM and DDM
[44]	The Bird Mating technique estimates the SDM parameters for PV solar array
[45]	Parameters extraction of three-diode PV models by Coyote optimization algorithm for PV modules
[46]	Parameters extraction of three-diode PV models by Elephant herd, cuckoo search and crow search optimizers for PV modules
[47]	This study provides an assessment of a modified three-diode against modified two-diode models of PV. Two methods are applied elephant herd optimizer and closed loop particle swarm optimization algorithm
[48]	An opposition-based sine cosine algorithm (SCA) was used to estimate the parameters of PV with different models. It based on the basic sine cosine optimization approach
[49]	The salp swarm optimization algorithm (SSA)was proposed and applied for extracting identifying the parameters of the electric model of PV. The optimal parameters were found using the double diode model of PV
[50]	Particle Swarm Optimization technique (PSO) was used to enhance the double diode model by using the experimental data to extract the proposed triple diode model. The model was applied to the large-scale industrial solar modules
[51]	Grey Wolf Optimizer (GWO) was proposed and developed to obtain an optimal model of PV. The approach considered the single diode model as the reference and accurate model of PV
[52]	A method called forensic optimization algorithm was proposed for three models of the parameter estimation of solar cells

of PN junction and consists of the partial short circuit (SC) current path near the cell's edges related to the semi-conductor layers and non-idealities and a series resistance which consider the effects of silicon and electrodes surfaces contact, electrodes resistance and the flowing current resistance.

Mathematically, the diode current 'I_{D1}' is given using Shockley diode equation:

$$I_{D1} = I_{s1}[e^{\left(\frac{V+IR_s}{\eta_1 V_T}\right)} - 1] \tag{1}$$

where I_{s1} represents the reverse saturation current, η_1 is the ideality factor of (D1), I is the output current of the cell, V is the output voltage of the cell, I_{D1} is the diode current, and R_s is the series resistance of the equivalent circuit of SDM. The

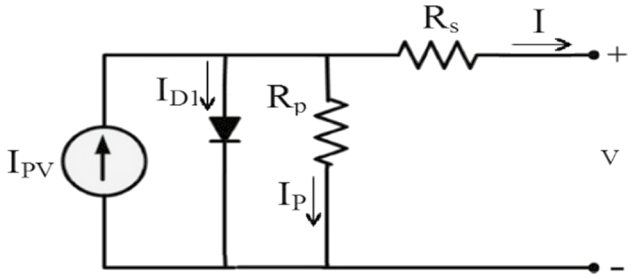

Fig. 1 Equivalent circuit for SDM of PV cell

thermal voltage of SDM 'V_T' is given ($V_T = K_B T/q$). K_B represents Boltzmann's constant ($K = 1.3806503 \times 10^{-23}$J/K), T is the operating temperature in Kelvin (K), and q is the electron charge ($q = 1.60217646 \times 10^{-19}$).

The load output current is calculated using (2).

$$I = I_{PV} - I_{D1} - I_P \tag{2}$$

where I_{PV} is the photons currents, I_P is the leakage current that passes through the shunt resistance which is calculated by:

$$I_P = \frac{V + IR_s}{R_P} \tag{3}$$

The (I–V) relation of SDM becomes:

$$I = I_{PV} - I_{s1}\left(e^{\left(\frac{V+IR_s}{\eta_1 V_T}\right)} - 1\right) - \frac{V + IR_s}{R_P} \tag{4}$$

In SDM, five unknown parameters ($I_{PV}, I_{s1}, \eta_1, R_PandR_s$) have to be estimated at their optimal values.

2.2 Double Diode Model

Practically, another additional diode is shunted to the current source considering the space charge recombination [54], compared with the SDM. The DDM equivalent circuit is shown in Fig. 2.

The additional new diode current is given as follows:

$$I_{D2} = I_{s2}[e^{\left(\frac{V+IR_s}{\eta_2 V_T}\right)} - 1] \tag{5}$$

where I_{s2} is the reverse saturation current, η_2 is the ideality factor of the second diode.

The output current I is now recalculated as follows:

$$I = I_{PV} - I_{D1} - I_{D2} - I_P \tag{6}$$

$$I = I_{PV} - I_{s1}\left(e^{\left(\frac{V+IR_s}{\eta_1 V_T}\right)} - 1\right) - I_{s2}\left(e^{\left(\frac{V+IR_s}{\eta_2 V_T}\right)} - 1\right) - \frac{V + IR_s}{R_P} \tag{7}$$

Equation (7) describes seven parameters of I–V relation which, ($I_{PV}, I_{s1}, I_{s2}, \eta_1, \eta_2, R_PandR_s$).

2.3 Triple Diode Model

In the triple-diode model (TDM), the influence of large leakage, and recombination in defect region are considered as in [12]. Therefore, the third diode is shunted with the DDM. Figure 3 shows the equivalent circuit of TDM.

Like SDM and DDM, the output current is calculated by applying KCL as follows:

$$I = I_{PV} - I_{s1}\left(e^{\left(\frac{V+IR_s}{\eta_1 V_T}\right)} - 1\right) - I_{s2}\left(e^{\left(\frac{V+IR_s}{\eta_2 V_T}\right)} - 1\right) - I_{s3}\left(e^{\left(\frac{V+IR_s}{\eta_3 V_T}\right)} - 1\right) - \frac{V + IR_s}{R_P} \tag{8}$$

where I_{s3} is the reverse saturation current and η_3 is the ideality factor of the third diode.

In the literature [55–57], seven parameters, I_{PV}, I_{s1}, I_{s2}, I_{s3}, η_3, R_P and R_s had been estimated for this model, while the other parameters remain constant as η_1 equal 1, η_2 was taken as 2, and $\eta_3 > 3$. In this work, nine parameters are estimated to get better results and enhance the accuracy of the higher models ($I_{PV}, I_{s1}, I_{s2}, I_{s3}, \eta_1, \eta_2, \eta_3, R_P$ and R_s).

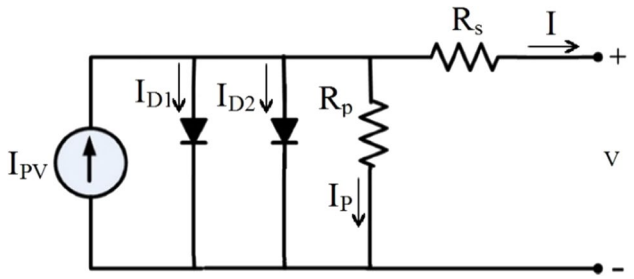

Fig. 2 Equivalent circuit for DDM of PV cell

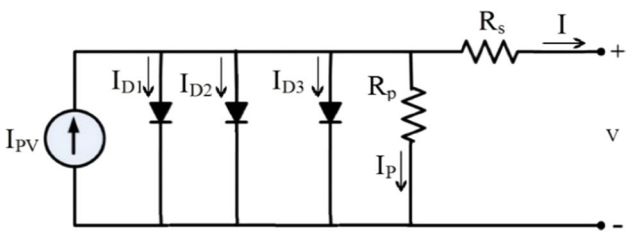

Fig. 3 Equivalent circuit for TDM of PV cell

3 Problem Formulation

The main goal of PV modeling is to minimize the difference between the data extracted using the proposed model and the measurements. This can be achieved by identify the unknown parameter of different PV models under a variety of operating conditions. The unknown parameters are estimated optimally in order to obtain accurate models as possible. It is required to use an efficient optimization algorithm to estimate various unknown parameters. In SDM, it is important to optimize five parameters ($I_{PV}, I_{s1}, \eta_1, R_P$ and R_s). Seven parameters in DDM have to be estimated ($I_{PV}, I_{s1}, I_{s2}, \eta_1, \eta_2, R_P$ and R_s). In TDM, nine parameters ($I_{PV}, I_{s1}, I_{s2}, I_{s3}, \eta_1, \eta_2, \eta_3, R_P$ and R_s) have to be optimized. It seems that the TDM is a complicated model and time consumed in estimation of its parameters; however it depicts the complicated behavior of different PV cells, especially the multi-crystalline cell. Using an efficient optimization algorithm give accurate results and minimize the execution time. Here in, the objective function is the mean root square error (MRSE). The error function is the difference between measured and modeled cell current. In this problem, the minimization of root means square error (RMSE) (9) is considered as the problem objective function (OF).

$$\text{MRSE} = \sqrt{\frac{1}{N}\sum_{k=1}^{N}\left[I(k) - I_{\exp}(k)\right]^2} \qquad (9)$$

$$\text{OF} = \min(\text{MRSE})$$

subject to:

$I_{PV}^{\min} \le I_{PV} \le I_{PV}^{\max}$

$I_{si}^{\min} \le I_{si} \le I_{si}^{\max}$ for $i = 1, 2,$ and 3

$\eta_i^{\min} \le \eta_i \le \eta_i^{\max}$ for $i = 1, 2,$ and 3

$i = 1$ for SDM,2 for DDM and 3 for TDM

$R_s^{\min} \le R_s \le R_s^{\max}$

$R_P^{\min} \le R_P \le R_P^{\max}$

where $I_{\exp}$ refers to the experimental current and N refers to the experimental data points.

According to the literature [8, 9, 39, 42–45], the upper and lower limits of different parameters are:

R_s is within the range[0 2], R_P is $\in$[50 5000], I_{s1}, I_{s2}, I_{s3} are $\in$[0 1E−12], η_1, η_2, η_3 are $\in$[1 5] and $I_{PV} \in [0\ 2\ I_{SC}]$ where I_{SC} is the short circuit current.

The proposed optimization algorithm, MPA, is used to estimate the optimal parameters of different models with minimum RMSE. The MPA code is built with the help of using MATLAB environment [46].

4 Proposed Marine Predator Algorithm

MPA is one of meta-heuristic optimization techniques. MPA is a nature-inspired from the marine predators' behavior. An optimal strategy between prey and predator is followed by MPA. This strategy allows predators to use an intelligent encounters rate policy and prey to utilize an optimal foraging strategy. MPA relies on the prey to predator speed ratio. The movement of prey and predator are simulated by Brownian motion and levy's flight. Spatial memories and advanced cognitive skills are utilized in many activities by marine predators such as food retrieval and recalling places where they are often finding the food. The optimization process is as follows:

4.1 Initialization of Population

MPA considered as a population-based algorithm with n space search. The initial population, X_0, is initialized randomly and based on allowable lower and upper limits of control variables (d search space), $X_{\max}$ and $X_{\min}$.

$$X_0 = X_{\min} + \text{rand} \times \left(X_{\max} - X_{\min}\right) \qquad (10)$$

where rand is uniformly distributed vector lies between 0 and 1.

4.2 Evaluate the Fitness and Construct Elite and Prey Matrices

The more intelligent in food search are considered to construct the most suitable solution. This solution is corresponding to the predator which sets up the Elite matrix to find the prey depending on information about prey's locations. Elite matrix is given for 'n' search agents and 'd' search space, as follows:

$$\text{Elite} = \begin{bmatrix} X_{1,1}^I & X_{1,2}^I \cdots & X_{1,d}^I \\ X_{2,1}^I & X_{2,2}^I \cdots & X_{2,d}^I \\ \vdots & \vdots & \vdots \\ \vdots & \vdots & \vdots \\ X_{n,1}^I & X_{n,2}^I \cdots & X_{n,d}^I \end{bmatrix} \qquad (11)$$

where the top predator vector $\overrightarrow{X^I}$ is repeated n times to represent the search agents for d dimension (control variables). Both prey and predator are considered search agent because both of them search for its own food. Thus another matrix called Prey matrix with the same dimension as Elite. The initialization found the initial Prey that the top predator construct Elite based on it and the updating of Elite is based on Prey locations.

$$\text{Prey} = \begin{bmatrix} X_{1,1} & X_{1,2} \cdots & X_{1,d} \\ X_{2,1} & X_{2,2} \cdots & X_{2,d} \\ \vdots & \vdots & \vdots \\ \vdots & \vdots & \vdots \\ X_{n,1} & X_{n,2} \cdots & X_{n,d} \end{bmatrix} \tag{12}$$

where $X_{i,j}$ represent ith prey at jth dimension.

4.3 MPA Phases

The optimization process takes three main phases after the initialization process of Prey matrices and Elite, according to three levels velocity ratio, high velocity ratio, unit velocity ratio and low velocity ratio. In first phase, the velocity of predator is slower than that of prey. The second phase occurs when the velocities of predator and prey are equal then we have a unity velocity ratio. Phase three indicates that predator is moving faster than prey. The action of predator and prey in these three phases is explained as follows:

4.3.1 Phase 1: High Velocity Ratio (Prey Moves in High Speed, ($v \geq 1$))

At the start of optimization process, the space between prey and predator is large and the prey moves in high speed. The best scenario of predator is not moving at all. This scenario takes place whileIter $\leq \frac{1}{3}$Max_Iter. Where, Iter is the current iteration, and maximum number of iteration is Max_Iter. The step size of prey and its position is formulated as follows:

$$\begin{aligned} \overrightarrow{\text{Stepsize}}_i &= \vec{R}_\text{b} \oplus \left(\overrightarrow{\text{Elite}}_i - \vec{R}_\text{b} \oplus \overrightarrow{\text{prey}}_i(t)\right), i = 1, \ldots, n \\ \overrightarrow{\text{prey}}_i(t+1) &= \overrightarrow{\text{prey}}_i(t) + P * \vec{R} \oplus \overrightarrow{\text{Stepsize}}_i \end{aligned} \tag{13}$$

where $\vec{R}_\text{b}$ is a normal distributed vector representing Brownian motion of prey, and the constant P has a value of 0.5. The vector $\vec{R}$ is randomly distributed values in range of [0,1]. The Prey's positions at time interval, '$t+1$', are updated using the calculated step size at the end of time interval 't'.

4.3.2 Phase 2: Unit Velocity Ratio ($v = 1$)

In this phase both prey and predator are looking for its prey. This occurs in the intermediate of the optimization process, while $\frac{1}{3}$Max_Iter $\leq$ Iter $\leq \frac{2}{3}$Max_Iter. In this phase the transition from exploration to exploitation takes place. Thus the population size is equally dividing for exploration and exploitation (i.e., one half tries to explore, while the other half of population exploits). The Levy's flight and Brownian movement are considered for the motion. The formulation of this phase is as follows:-

For exploration stage (the first half of population):

$$\begin{aligned} \overrightarrow{\text{Stepsize}}_i &= \vec{R}_\text{L} \oplus \left(\overrightarrow{\text{Elite}}_i - \vec{R}_\text{L} \oplus \overrightarrow{\text{prey}}_i(t)\right), i = 1, \ldots, n/2 \\ \overrightarrow{\text{prey}}_i(t+1) &= \overrightarrow{\text{prey}}_i(t) + P * \vec{R} \oplus \overrightarrow{\text{Stepsize}}_i \end{aligned} \tag{14}$$

The vector, $\vec{R}_\text{L}$, represents the Levy distribution of movement and has random numbers. The production of $\vec{R}_\text{L}$ and the prey represent the levy movement. Updating the prey movement is considered through adding the step size to the position of prey. The best value of P was found as 0.5. The step size of this stage is small to enable preys to exploit in the second half of the population.

For exploitation stage (the second half of population):

$$\begin{aligned} \overrightarrow{\text{Stepsize}}_i &= \vec{R}_b \oplus \left(\vec{R}_b \oplus \overrightarrow{\text{Elite}}_i - \overrightarrow{\text{prey}}_i(t)\right), i = n/2, \ldots, n \\ \overrightarrow{\text{prey}}_i(t+1) &= \overrightarrow{\text{prey}}_i(t) + P * \text{CF} \oplus \overrightarrow{\text{Stepsize}}_i \end{aligned} \tag{15}$$

The production of $\vec{R}_\text{b}$ and Elite represent the Brownian movement of Elite. Prey updates its position according to predator movement and an adaptive factor, CF, with a value equal to $\text{CF} = \left(1 - \frac{\text{Iter}}{\text{Max}_\text{Iter}}\right)^{(2\text{Iter}/\text{Max\_Iter})}$.

4.3.3 Phase 3: Low Velocity Ratio (Prey Moves In Low Speed, ($v = 0.1$)

In this phase predator moves faster than prey and it prefers to move in Levy's flight motion. In This phase predator exploits its prey. This stage occurs whileIter $> \frac{2}{3}$Max_Iter. Prey updates its position based on predator.

$$\begin{aligned} \overrightarrow{\text{Stepsize}}_i &= \vec{R}_\text{L} \oplus \left(\vec{R}_\text{L} \oplus \overrightarrow{\text{Elite}}_i - \overrightarrow{\text{prey}}_i(t)\right), i = 1, \ldots, n \\ \overrightarrow{\text{prey}}_i(t+1) &= \overrightarrow{\text{Elite}}_i + P * \text{CF} \oplus \overrightarrow{\text{Stepsize}}_i \end{aligned} \tag{16}$$

4.4 FADs' Effect

The predators alter their manner according to environmental conditions. One of the most important conditions is "Fish Aggregating Devices" (FADs) effect which motivates predators to find different areas with different preys' distribution and concentration. FADs is considered as local optima. FADs = 0.2 which represents the probability of FADs effect on optimization process. The effect of FADs on prey's positions is given as in Eq. (17)

$$\overrightarrow{\text{prey}}_i = \begin{cases} \overrightarrow{\text{prey}}_i + \text{CF}\left[\vec{X}_\text{min} + \vec{R} \oplus (\vec{X}_\text{max} - \vec{X}_\text{min})\right] \oplus \overrightarrow{U} & \text{if } r \leq \text{FADs} \\ \overrightarrow{\text{prey}}_i + [\text{FADs}(1-r) + r]\left(\overrightarrow{\text{prey}}_{r1} - \overrightarrow{\text{prey}}_{r2}\right) & \text{if } r > \text{FADs} \end{cases} \tag{17}$$

where the binary vector $\overrightarrow{U}$ contains 0 and 1. It is generated randomly in the range [0,1], then it changes its array to zero if the array is less than 0.2 and the array becomes ones if

the generated array is greater than 0.2. The indices $r1$ and $r2$ indicate random indices of prey matrix.

4.5 Memory Saving of MPA

Memory saving in MPA reflects the predators' good memory that allows them to remember the best search food locations. The fitness of updated prey is evaluated in this stage for each solution at time interval $(t+1)$ and compared to the corresponding one at the previous time interval t. Elite matrix is updated by deciding the best fitness obtained. The flowchart of MPAbased approach is illustrated in Fig. 4.

5 Results and Discussion

The performance of proposed MPA is verified by estimating the parameters of two case studies of PV cells with three models (SDM, DDM and TDM):

Case study 1: In this study case, R.T.C. France silicon solar cell with 57 mm diameter commercial is considered to be verified. The experimental (I–V) data of case study at normal operating condition (1000 W/m^2 at 33 °C) are taken from the literature [31].

Case study 2: In the second case, multi-crystalline silicon solar cell Q6-1380witharea of 7.7 cm^2 is taken to investigate the most accurate model representing its behavior. The cell operates under room temperature (27 °C) and low irradiation level (98.4 W/m^2) [9]. The experimental dataset is taken from the literature [9].

To test the effectiveness of the proposed MPA-based parameter estimation technique, it has been compared to four well known competitive optimization algorithms in the field of solar cell parameters estimation. The competitive algorithms are SCA [48], SSA [49], PSO [50] and GWO [51]. To make the comparison fair, all of search agents of the competitive algorithms are set at 100 agents and the maximum number of iterations is set at 400. All results obtained in this research are carried out using the MATLAB

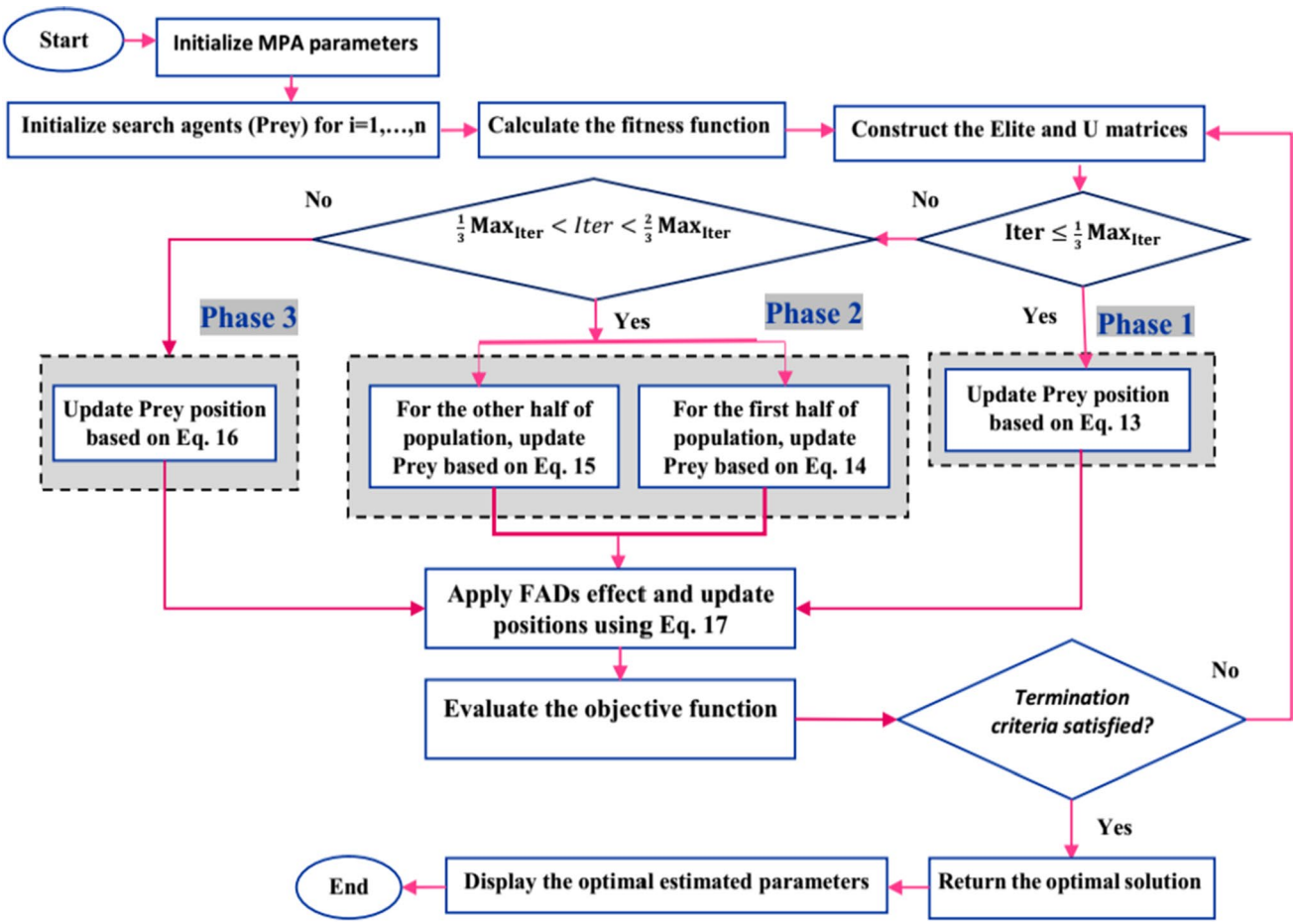

Fig. 4 Flowchart of the proposed MPAbased-parameter estimation technique

R2016b software on a PC with Intel(R) Core (TM)i3-CPU M370@2.4 GHz 3 GB (RAM).

The variation of objective function (RMSE) over many runs of the algorithm (30–100 runs) can be used to investigate the robustness of any algorithm. A lower change in objective function over runs indicates that the algorithm is more robust. To confirm the robustness of the proposed MPA, about 100 individual runs for different PV models, SDM, DDM and TDM, recorded at normal and low radiation operating conditions, respectively.

5.1 Simulation Results for Single Diode Model

- *Case study 1*

For SDM, the comparison results including estimated parameters and RMSE are shown in Table 2. It is clear that MPA provides the lowest RMSE (8.43854E−4) among the competitive algorithms, followed by SCA [48], SSA [49], PSO [50]. The RMSE is considered as the best index used to represent the accuracy of methods. The convergence rates of MPA compared with GWO, PSO, SSA and SCA algorithms are shown in Fig. 5a. The robustness of the proposed algorithm *has* been tested by checking the variation of the RMSE over 100 runs of the algorithm. Figure 5b presents the robustness of the proposed MPA compared with GWO and PSO for SDM. The convergence rate and robustness emphasize the effectiveness of MPA. For further validation of the quality of the estimated results, the extracted parameters have been used to reconstruct *I–V* and *P–V* curves, as illustrated in Fig. 6. It is noticed that the estimated data obtained by the proposed MPA is highly closest to the measured data which prove the high accuracy of estimated parameters. In this case, the RMSE has the lowest value of (8.43854E−4) compared with SCA, SSA, PSO, and GWO which have 9.26567E−4, 8.45486E−4, 8.45724E−4 and 8.50301E−4, respectively.

- *Case study 2*

In this case, the PV operates under low irradiance. The accuracy and performance of MPA are checked to prove the accuracy of the extracted model. Table 3 introduces the simulation results compared to the selected competitive algorithm. The convergence rate and robustness are presented in Fig. 7. Also, the optimization parameters are used to reconstruct *I–V* and P–V characteristics as shown in Fig. 8. Therefore, Table 3, Figs. 7 and 8, assure the high robustness of the proposed MPA. In this case, the RMSE has the lowest value of (1.611E−05) compared with SCA, SSA, PSO, and GWO which 3.86E−05, 3.86E−05, 2.10E−05 and 1.69E−05, respectively.

Table 2 Comparison of simulation results for SDM (Case study #1)

Algorithm	R_P (Ω)	R_S (Ω)	η_1	I_{S1} (A)	I_{PV} (A)	RMSE	Rank
MPA	51.79484084	0.037214598	1.465687442	2.80E−07	0.76078	8.43854E−4	1
SCA [48]	50.96919115	0.038069364	1.451390692	2.42E−07	0.76078	9.26567E−4	5
SSA [49]	51.6315017	0.037121619	1.467467157	2.85E−07	0.76078	8.45486E−4	2
PSO [50]	52.50334238	0.037071124	1.46900025	2.89E−07	0.76078	8.45724E−4	3
GWO [51]	51.80331115	0.037212697	1.465734872	2.80E−07	0.76078	8.50301E−4	4

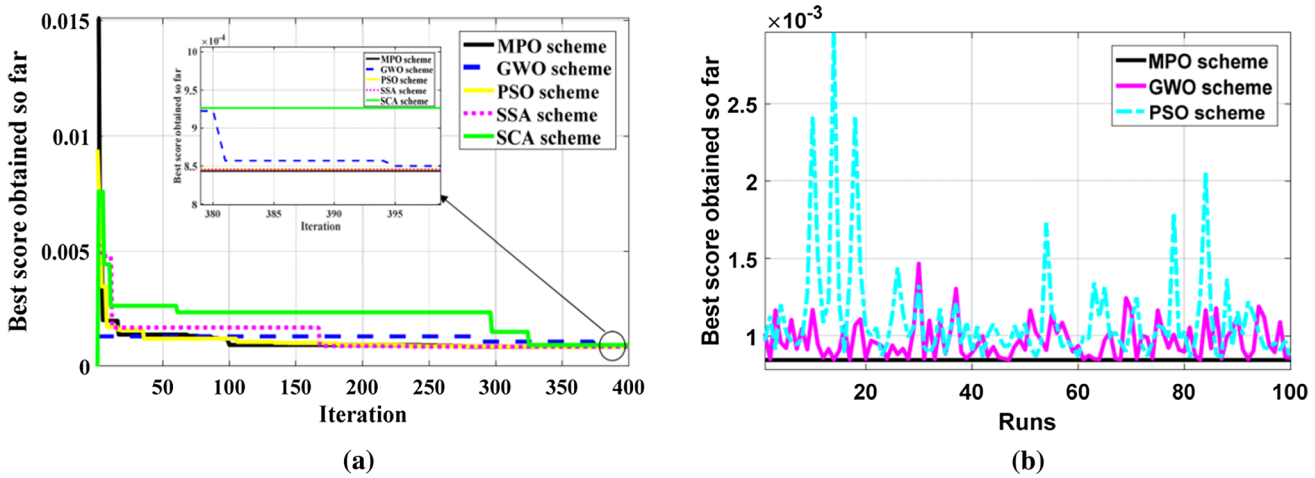

Fig. 5 Comparison of performance rates for SDM (Case Study #1), **a** Convergence rates and **b** Robustness characteristic

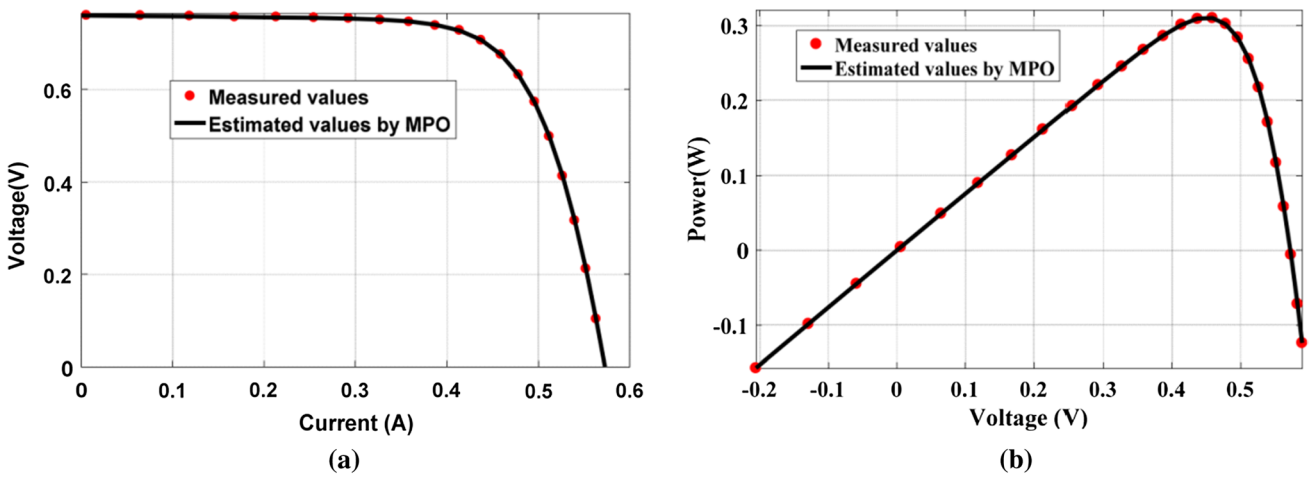

Fig. 6 Comparison between measured and estimated data using the proposed MPA for SDM (Case study#1), **a** *I–V* curve and **b** P–V curve

Table 3 Comparison of simulation results for SDM (Case study #2)

Algorithm	R_P (Ω)	R_S (Ω)	η_1	I_{S1} (A)	I_{PV} (A)	RMSE	Rank
MPA	971.351	0.45	3.389204263	9.29E−05	0.019349731	1.611E−05	1
SCA [48]	971.351	0.45	3.513808978	0.000109144	0.019408303	3.86E−05	5
SSA [49]	1163.510619	0.5541	3.429712352	9.74E−05	0.019353862	2.10E−05	4
PSO [50]	971.351	0.45	3.389208419	9.29E−05	0.019349734	1.612E−05	2
GWO [51]	971.351	0.45	3.389190436	9.29E−05	0.019349726	1.69E−05	3

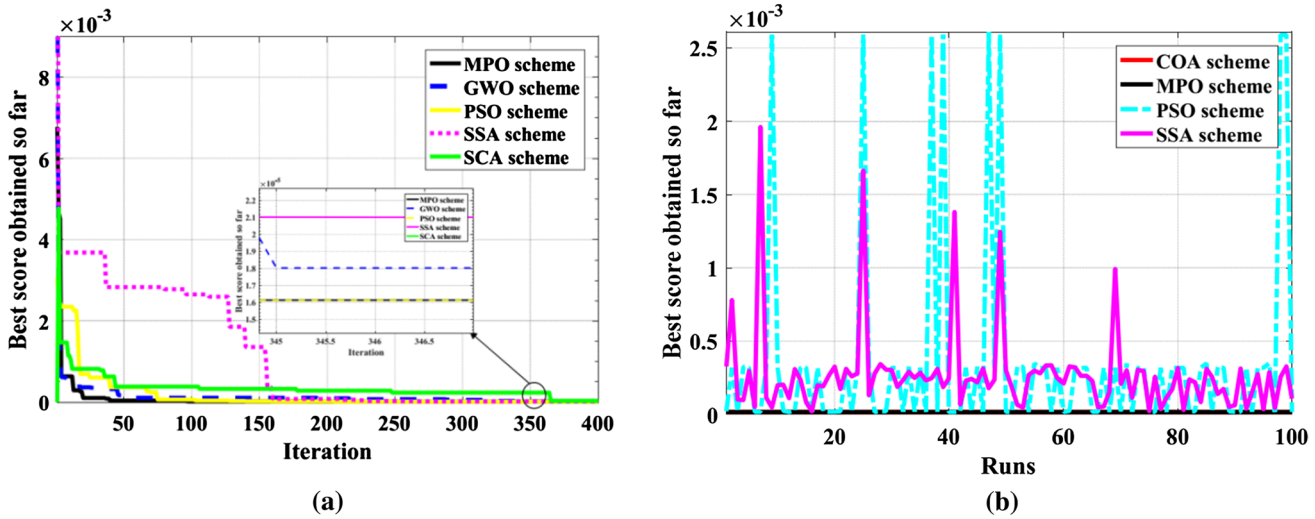

Fig. 7 Comparison of performance rates for SDM (Case Study #2), **a** Convergence rates and **b** Robustness characteristic

5.2 Simulation Results for Double Diode Model

- *Simulation results of Case study 1*

For DDM, the simulated results compromising optimal parameters and RMSE are shown in Table 4. As shown, MPA provides the lowest RMSE (7.592E−4), followed by PSO, GWO, SSA, and SCA. Figure 9a represents the convergence rates of MPA with the four competitive algorithms GWO, PSO, SSA and SCA. The robustness characteristic of the MPA and competitive algorithms is illustrated in Fig. 9b. All of these results again confirm the effectiveness of MPA. V–I curve, for measured and calculated values, is shown in Fig. 10, which emphasizes the high closeness between the

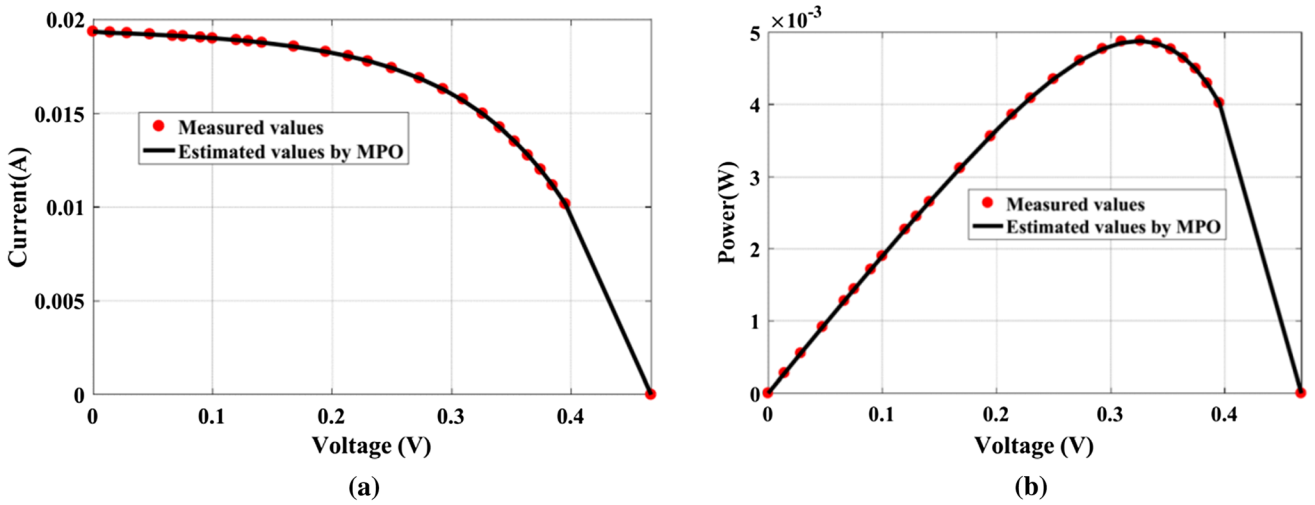

Fig. 8 Comparison between measured and estimated data using the proposed MPA for SDM (case study#1), **a** *I–V* curve and **b** P–V curve

Table 4 Optimal PV estimated parameters of competitive optimization methods for DDM (Case study #1)

Algorithm	R_P (Ω)	R_S (Ω)	η_1	η_2	I_{S1} (A)	I_{S2} (A)	I_{PV} (A)	RMSE	Rank
MPA	62.4591	0.03869	1.39036	2.56454	1.18E−07	1.00E−05	0.76077	7.592E−4	1
SCA [48]	50.0000	0.03772	1.45478	2.76999	2.51E−07	9.37E−11	0.76077	13.14E−4	5
SSA [49]	61.8183	0.03677	1.92948	1.44999	7.10E−07	2.22E−07	0.76077	9.150E−4	4
PSO [50]	55.3354	0.03752	1.45191	3.32821	2.41E−07	1.00E−05	0.76077	8.071E−4	2
GWO [51]	50.8790	0.03723	1.46497	1.73253	2.78E−07	1.39E−09	0.760888	8.218E−4	3

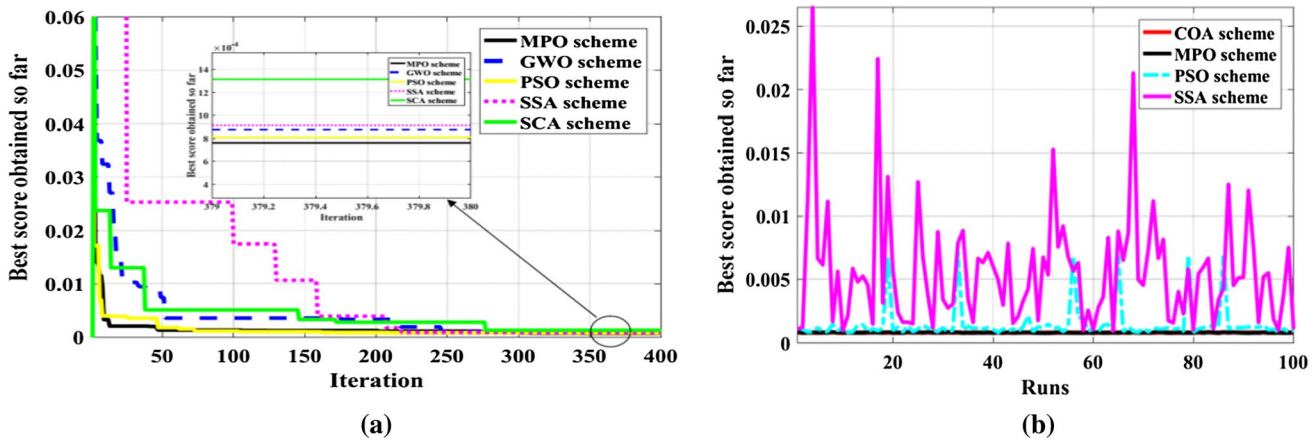

Fig. 9 Comparison of performance rates for DDM (Case Study #1). **a** Convergence rates and **b** robustness characteristic

estimated and experimental *I–V* curve. Based on Table 4, the MPA has the first rank followed by PSO, GWO, SSA then SCA, respectively.

- *Simulation results of Case study 2*

In this case, the simulation results compared to the competitive algorithms are introduced in Table 5. The least value of RMSE is obtained with the proposed MPA (1.461E−05) compared to 1.462E−05, 1.48E−05, 1.56E−05, and 5.50E−05 for PSO, SSA, GWO, and SCA, respectively.

5.3 Simulation Results for Three Diode Model

Similarly, to the previous two models, the proposed MPA is developed for TDM and the obtained results are assessed

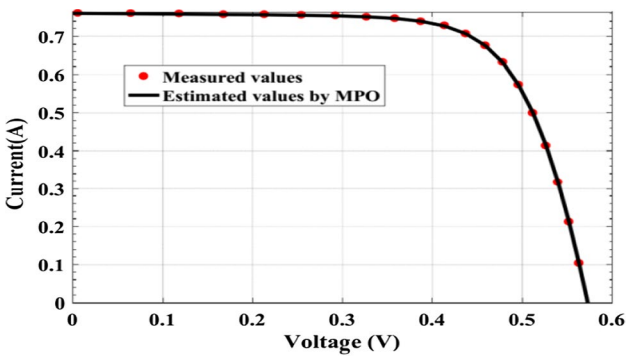

Fig. 10 Performance of I–V for DDM using the proposed MPA (Case study #1)

compared with several published studies in the literature. In both studied cases, TDM is considered as the most accurate model dealing with the complicated behavior of PV cells, especially multi-crystalline PV cell. Tables 6 and 7 show the optimal PV estimated parameters and the ranking of RMSE for MPA compared with the competitive optimization methods for TDM for Case study 1 and 2, respectively. It is observed that MPA has the least RMSE for the two studied cases with PSO, GWO, SSA and SCA. The obtained results assure the high capability of the proposed MPA.

For Case study1, the RMSE via MPA equals 8.43854E−4, 7.592E−4, and 7.592E−4 for SDM, DDM, and TDM (Tables 2, 4, and 6), respectively. These results emphasizes that DDM and TDM are more accurate than TDM.

For case study 2, as the physical behavior of multi-crystalline PV cell is more complicated, TDM is the most accurate model. The results obtained from Tables 3, 5, and 7 confirm the accuracy of TDM as the RMSE values are 1.461E−05 for TDM, 1.46E−05 for DDM, and 1.611E−05 via SDM.

Figure 11 shows the high closeness between the experimental and estimated *I–V* and *P–V* curves for Case study 1 and 2. The solution quality is proved in Fig. 12 through the fast convergence rates and the robustness of the proposed MPA compared to other competitive algorithms. Moreover, the values of RMSE obtained for the three models are illustrated in Fig. 12c, d. these figures confirm again the accuracy of DDM and TDM and that MPA outperforms all compared algorithms. The previous results prove the high capability of the proposed MPA for optimizing the considered parameter estimation problem of solar cells at normal and low radiation Case study 1 and 2) (Fig. 13).

Table 5 Optimal PV estimated parameters of competitive optimization methods for DDM (Case study #2)

Algorithm	R_P (Ω)	R_S (Ω)	η_1	η_2	I_{S1} (A)	I_{S2} (A)	I_{PV} (A)	RMSE	Rank
MPA	950	1	2.595	4.047	1.00E−05	9.85E−05	0.019391	1.46E−05	1
GWO [51]	950.7	0.642796	2.566	3.660	5.25E−06	9.59E−05	0.019368	1.56E−05	4
PSO [50]	950	0.955747	2.615	3.956	1.00E−05	9.46E−05	0.019386	1.462E−05	2
SSA [49]	959.7	0.722057	2.662	3.833	9.77E−06	9.56E−05	0.019374	1.48E−05	3
SCA [48]	1100	0.711326	1	3.594	3.40E−11	1.144E−4	0.019423	5.50E−05	5

Table 6 Optimal PV estimated parameters of competitive optimization methods for TDM for Case study 1

Algorithm	R_P (Ω)	R_S (Ω)	η_1	η_2	η_3	I_{S1} (A)	I_{S2} (A)	I_{S3} (A)	I_{PV} (A)	RMSE	Rank
MPA	64.998	0.0391	1.376	1.9985	2.69	1.00E−07	2.76E−12	1.54E−05	0.76080184	7.561E−4	1
GWO [51]	61.139	0.0395	1.367	2.997	2.62	9.02E−08	5.11E−12	1.32E−05	0.760876	7.8E−4	3
PSO [50]	65	0.0391	1.376	4	2.69	1.00E−07	1.00E−11	1.55E−05	0.760776	7.562E−4	2
SSA [49]	61.613	0.0398	1.357	1.0652	2.79	8.00E−08	1.78E−12	2.12E−05	0.760876	8.14E−4	4
SCA [48]	64.019	0.04	1.372	1.5599	3.66	9.83E−08	9.99E−13	7.08E−05	0.760776	9.77E−4	5

Table 7 Optimal PV estimated parameters of competitive optimization methods for TDM for Case study 2

Algorithm	R_P (Ω)	R_S (Ω)	η_1	η_2	η_3	I_{S1} (A)	I_{S2} (A)	I_{S3} (A)	I_{PV} (A)	RMSE	Rank
MPA	607.876	0.7579	1.9380	3.215	4.949	1.00E−12	6.81E−05	5.71E−08	0.0193951	1.42E−05	1
GWO [51]	723.427	1.5467	1.99999	2.000	3.508	7.08E−07	1.07E−09	7.33E−05	0.0194251	1.44E−05	2
PSO [50]	600	0.4	2	3.291	3.5	1.00E−12	7.97E−05	1.00E−12	0.01938786	1.56E−05	4
SSA [49]	680.376	1.8167	1.98669	3.372	4.324	7.20E−07	4.83E−05	2.38E−05	0.01944742	1.48E−05	3
SCA [48]	661.879	0.4249	1.17916	2	3.5	1.74E−12	2.07E−07	9.97−05	0.01937818	4.09E−05	5

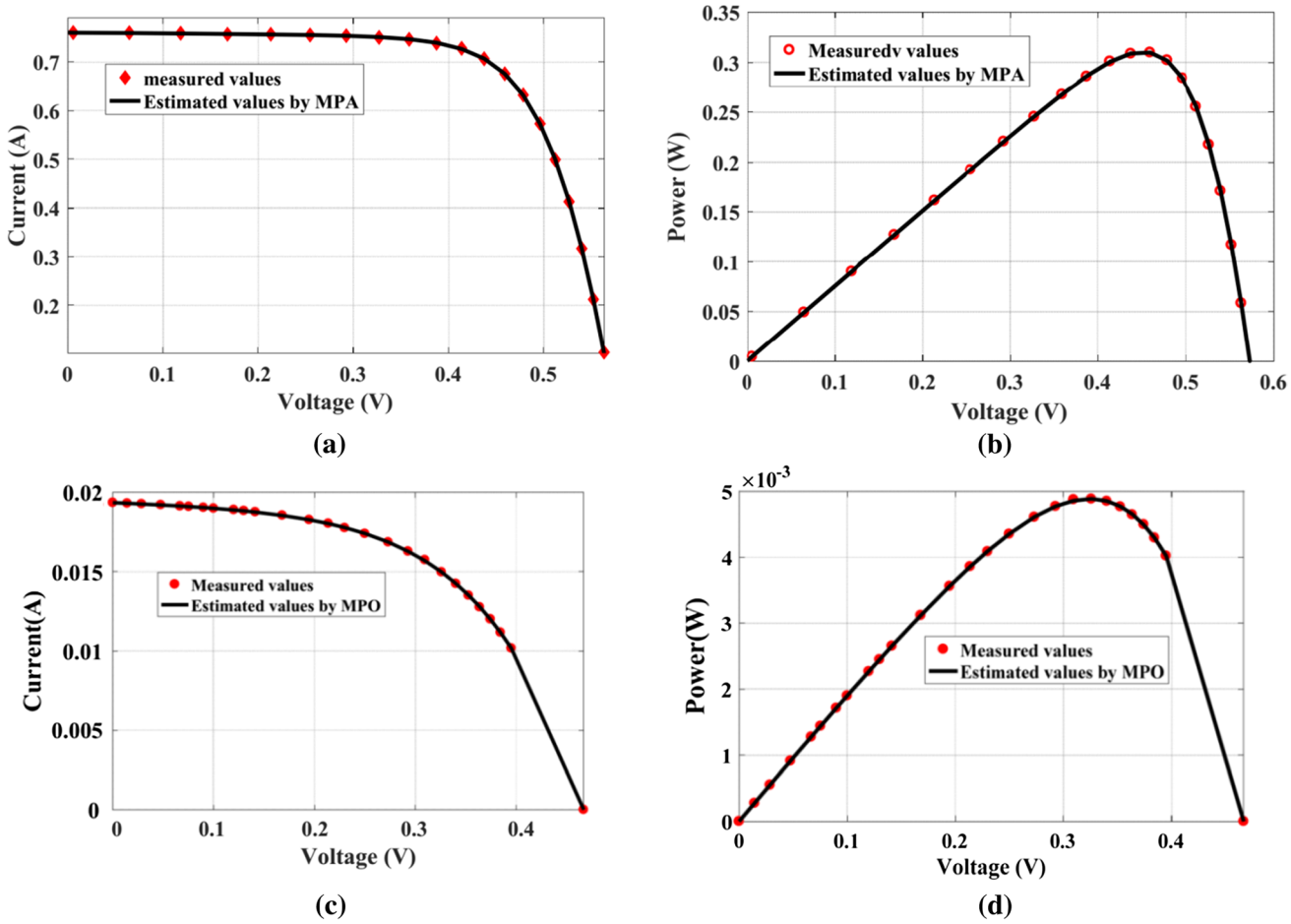

Fig. 11 Closeness between estimated and experimental dataset for Case study 1 and 2 **a**, **c**: (I–V) curves, **b**, **d** (P–V) curves

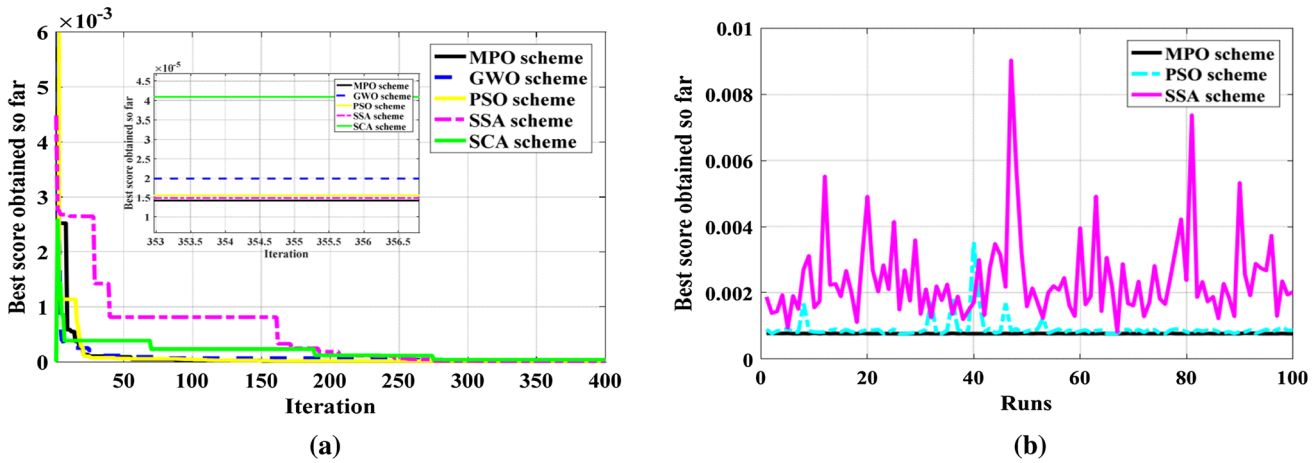

Fig. 12 Convergence rates and robustness of TDM using the proposed MPA compared with competitive algorithms **a** convergence rate for Case study 2, **b** robustness for Case study 2

5.4 Statistical Analysis

The statistical analysis compromising best, worst, average and standard deviation of RMSE, is applied over 100 independent runs to the selected studied cases with the three models of PV. The statistical analysis can confirm the average accuracy and reliability of the proposed algorithm. Tables 8 and 9 introduce the statistical analysis of Case study 1 and 2,

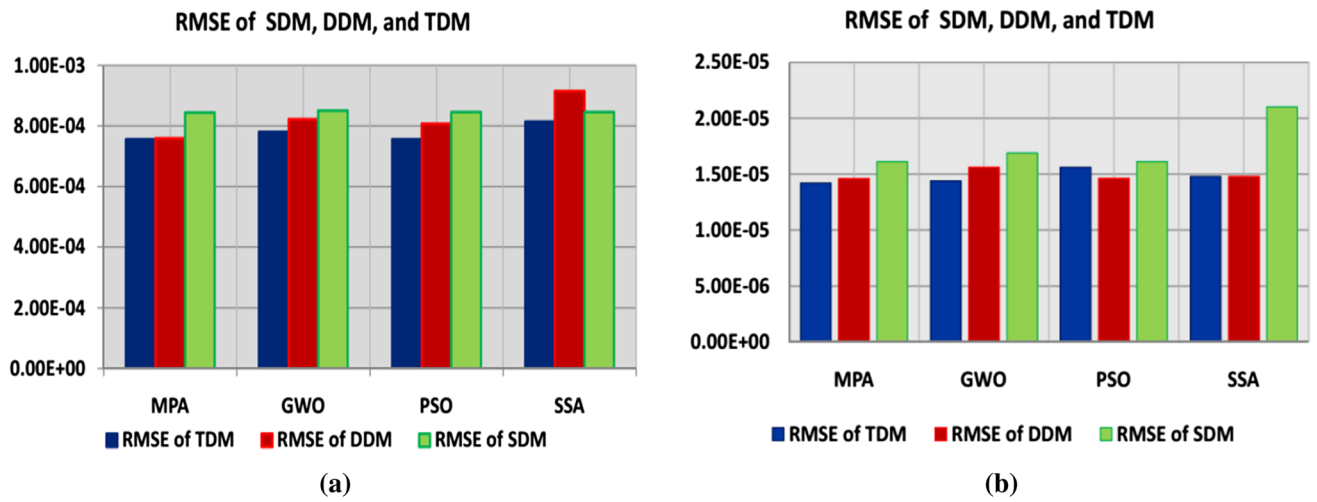

Fig. 13 Comparison of RMSE using the proposed MPA compared with competitive algorithms **a** RMSE of different models for Case study 1, and **b** RMSE of different models for Case study 2

respectively. It can be noticed that the proposed MPA-based estimated parameters method has the best RMSE over all cases and models. Moreover, TDM has the best RMSE as it is 7.56E−4 in Case 1 and 1.42E−5 for Case2.

The Standard deviation indicates the MPA can realize higher reliability in parameter estimation problem, as it observed from Table 8 that MPA gets the best standard deviation (3.56E−10, 1.86E−5, and 4.37E−6 for SDM, DDM, TDM, respectively). Table 9, also, emphasizes the high reliability of MPA compared to the other methods as it realizes the best recorded standard deviation (5.07E−12, 2.00E−7, and 2.04E−7 corresponding to SDM, DDM, and TDM). The PSO achieve the second best RMSE and standard deviation in Case 1. In Case 2, the second best RMSE with SDM and DDM is via PSO, while GWO realize the second best RMSE with TDM. Also, GWO achieve the second-best standard deviation with SDM and TDM.

From all discussions, it can be concluded that the proposed MPA outperforms the four competitive algorithms. It is accurate and reliable in extracting optimal parameters of different models and in variety of operating conditions.

6 Conclusions

In this work, a new MPA has been developed to estimate the optimal parameters of three PV models at normal and low radiations operating conditions. These models are single-, double- and three-diode PV models. The normal operating condition has been employed on the 57 mm diameter commercial (R.T.C. France) silicon solar cell while the second case was carried out on a MCSSC of area 7.7 cm^2 from Q6-1380 irradiated by low levels. The main goal of this study is to estimate an accurate and reliable PV model for any commercial panel under any operating conditions. This model of PV helps the studying of various real operating systems such as stand-alone microgrid, grid-connected microgrid, PV pumping system. The simulation results assure robustness of the proposed MPA for accurate parameters achievement with good and fast convergence. Also, the estimated performance curves, for current and power versus the cell voltage, obtained by the proposed algorithm are very close to the experimental date for the two studied operating conditions. The convergence rate has been used as an assessment criterion that is considered in this study. The convergence curves assure the highest and fast rates to reach the steady solutions for the studied cases compared with several optimizers in the literature. These figures expose the good convergence rates of MPA. Furthermore, the proposed MPA has achieved the best RMSE, the lower standard deviation overall the models and with the two studied cases. Therefore, this method is highly outperformance compared with GWO, SSA, PSO, and SCA. It was proven that the MPA leads to high accuracy solutions supported by the lowest RMSE and high reliability in terms of lowest standard deviations given for all tested cases. MPA can be considered as a promising and distinct optimization tool, especially in case of nonlinear complex optimization situations.

In the future research, advanced models to represent hysteresis behavior of the solar cell will be considered. Also, the MPA will be intended to solve several problems such as optimal power flow, unit commitment, economic load dispatch, parameter estimation of poly phase induction machines, fuel cell and battery energy storage and energy hub issues. In the area of solution methodology, when developing MPA in joint with other optimization methods such as PSO, SSA, SCA and GWO then it will produces an new hybrid optimization algorithm that combines the merits of the two jointed algorithms.

Table 8 Statistical analysis for different models of PV (Case study 1)

Algorithm	Best OF			Worst OF			Average OF			Standard deviation Standard deviation		
	SDM	DDM	TDM	SDM	DDM	TDM	SDM	DDM	TDM	SDM	DDM	TDM
MPA	**8.43854E−4**	**7.59E−4**	**7.561E−4**	**8.43856E−4**	**8.43E−4**	**7.74E−4**	**8.43854E−4**	**8E−4**	**7.6E−4**	**3.56E−10**	**1.86E−5**	**4.37E−6**
GWO [51]	8.50E−4	8.22E−4	7.8E−4	8.50E−4	1.84E−3	2.98E−3	1.083E−3	1.13E−3	9.78E−4	1.337E−4	1.874E−4	3.5E−4
PSO [50]	8.457E−4	8.07E−4	7.562E−4	8.457E−4	7.22E−3	3.52E−3	9.705E−4	1.45E−3	9.1E−4	1.217E−4	1.40E−3	3.36E−4
SSA [49]	8.454E−4	9.15E−4	8.14E−4	8.454E−4	2.65E−2	9.03E−3	1.113E−3	5.63E−3	2.41E−3	3.354E−4	4.51E−3	1.298E−3
SCA [48]	9.26E−4	13.15E−4	9.77E−4	3.05E−3	1.18E−2	6.31E−3	1.64E−3	3.47E−	2.84E−3	4.24E−4	1.75E−3	1.02E−3

Bold indicates the best values by the proposed algorithm

Table 9 Statistical analysis for different models of PV (Case study 2)

Algorithm	Best OF			Worst OF			Average OF			Standard deviation		
	SDM	DDM	TDM	SDM	DDM	TDM	SDM	DDM	TDM	SDM	DDM	TDM
MPA	1.61E−5	1.46E−5	1.42E−5	1.61E−5	1.57E−5	1.52E−5	1.61E−5	1.48E−5	1.45E−5	5.07E−12	2.00E−7	2.04E−7
GWO [51]	1.69E−5	1.56E−5	1.44E−5	5.77E−5	2.23E−4	3.76E−4	2.42E−5	3.28E−5	3.12E−5	8.06E−6	2.42E−5	3.62E−5
PSO [50]	1.61E−5	1.46E−5	1.56E−5	2.61E−3	2.36E−4	2.61E−3	3.58E−4	2.28E−5	7.32E−4	6.78E−4	2.25E−5	1.01E−3
SSA [49]	2.10E−5	1.48E−5	1.48E−5	1.96E−3	5.05E−5	2.09E−4	2.73E−4	2.18E−5	4.65E−5	3.02E−4	6.79E−6	4.39E−5
SCA [48]	3.86E−5	5.50E−5	4.09E−5	2.59E−3	4.39E−4	9.36E−4	8.30E−4	1.56E−4	1.33E−4	1.10E−3	7.69E−5	1.41E−4

References

1. Ishaque, K.; Salam, Z.; Mekhilef, S.; Shamsudin, A.: Parameter extraction of solar photovoltaic modules using penalty-based differential evolution. Appl. Energy **99**, 297–308 (2012)
2. Bonanno, F.; Capizzi, G.; Graditi, G.; Napoli, C.; Tina, G.M.: A radial basis function neural network based approach for the electrical characteristics estimation of a photovoltaic module. Appl. Energy. **97**, 956–961 (2012)
3. Sandrolini, L.; Artioli, M.; Reggiani, U.: Numerical method for the extraction of photovoltaic module double-diode model parameters through cluster analysis. Appl. Energy. **87**, 442–451 (2010)
4. Amrouche, B.; Guessoum, A.; Belhamel, M.: A simple behavioural model for solar module electric characteristics based on the first order system step response for MPPT study and comparison. Appl. Energy. **91**, 395–404 (2012)
5. Orioli, A.; Di Gangi, A.: A procedure to calculate the five-parameter model of crystalline silicon photovoltaic modules on the basis of the tabular performance data. Appl. Energy **102**, 1160–1177 (2013)
6. Chenouard, R.; El-Sehiemy, R.A.: An interval branch and bound global optimization algorithm for parameter estimation of three photovoltaic models. Energy Convers. Manag. (2020). https://doi.org/10.1016/j.enconman.2019.112400
7. Abido, M.A.; Khalid, M.S.; Worku, M.Y.: An efficient ANFIS-based PI controller for maximum power point tracking of PV systems. Arab. J. Sci. Eng. **40**, 2641–2651 (2015). https://doi.org/10.1007/s13369-015-1749-z
8. Dash, S.K.; Ray, P.K.: Design and modeling of single-phase PV-UPQC scheme for power quality improvement utilizing a novel notch filter-based control algorithm: an experimental approach. Arab. J. Sci. Eng. **43**, 3083–3102 (2018). https://doi.org/10.1007/s13369-018-3116-3
9. Zaky, A.A.; Ibrahim, M.N.; Rezk, H.; Christopoulos, E.; El Sehiemy, R.A.; Hristoforou, E.; Kladas, A.; Sergeant, P.; Falaras, P.: Energy efficiency improvement of water pumping system using synchronous reluctance motor fed by perovskite solar cells. Int. J. Energy Res. **44**, 11629–11642 (2020). https://doi.org/10.1002/er.5788
10. El-Ela, A.A.A.; El-Sehiemy, R.A.; Kinawy, A.M.; Ali, E.S.: Optimal placement and sizing of distributed generation units using different cat swarm optimization algorithms. In: 2016 18th International Middle-East Power Systems Conference, MEPCON 2016—Proceedings (2017)
11. Abou El-Ela, A.A.; El-Sehiemy, R.A.; Ali, E.S.; Kinawy, A.M.: Minimisation of voltage fluctuation resulted from renewable energy sources uncertainty in distribution systems. IET Gener. Transm. Distrib. (2019). https://doi.org/10.1049/iet-gtd.2018.5136
12. Nishioka, K.; Sakitani, N.; Uraoka, Y.; Fuyuki, T.: Analysis of multicrystalline silicon solar cells by modified 3-diode equivalent circuit model taking leakage current through periphery into consideration. Sol. energy Mater. Sol. cells. **91**, 1222–1227 (2007)
13. Kassis, A.; Saad, M.: Analysis of multi-crystalline silicon solar cells at low illumination levels using a modified two-diode model. Sol. Energy Mater. Sol. Cells. (2010). https://doi.org/10.1016/j.solmat.2010.06.036
14. Chan, D.S.H.; Phang, J.C.H.: Analytical methods for the extraction of solar-cell single-and double-diode model parameters from IV characteristics. IEEE Trans. Electron Devices. **34**, 286–293 (1987)
15. Ishaque, K.; Salam, Z.; Taheri, H.: others: Modeling and simulation of photovoltaic (PV) system during partial shading based on a two-diode model. Simul. Model. Pract. Theory. **19**, 1613–1626 (2011)
16. Elbaset, A.A.; Ali, H.; Abd-El Sattar, M.: Novel seven-parameter model for photovoltaic modules. Sol. Energy Mater. Sol. Cells **130**, 442–455 (2014)
17. Bayoumi, A.S.; El-Sehiemy, R.A.; Mahmoud, K.; Lehtonen, M.; Darwish, M.M.F.: Assessment of an improved three-diode against modified two-diode patterns of MCS solar cells associated with soft parameter estimation paradigms. Appl. Sci. (2021). https://doi.org/10.3390/app11031055
18. Jadidbonab, M.; Mohammadi-Ivatloo, B.; Marzband, M.; Siano, P.: Short-term self-scheduling of virtual energy hub plant within thermal energy market. IEEE Trans. Ind. Electron. (2021). https://doi.org/10.1109/TIE.2020.2978707
19. Gholinejad, H.R.; Loni, A.; Adabi, J.; Marzband, M.: A hierarchical energy management system for multiple home energy hubs in neighborhood grids. J. Build. Eng. (2020). https://doi.org/10.1016/j.jobe.2019.101028
20. Nazari-Heris, M.; Mirzaei, M.A.; Mohammadi-Ivatloo, B.; Marzband, M.; Asadi, S.: Economic-environmental effect of power to gas technology in coupled electricity and gas systems with price-responsive shiftable loads. J. Clean. Prod. (2020). https://doi.org/10.1016/j.jclepro.2019.118769
21. Pazouki, S.; Haghifam, M.R.; Moser, A.: Uncertainty modeling in optimal operation of energy hub in presence of wind, storage and demand response. Int. J. Electr. Power Energy Syst. (2014). https://doi.org/10.1016/j.ijepes.2014.03.038
22. Vahid-Pakdel, M.J.; Nojavan, S.; Mohammadi-ivatloo, B.; Zare, K.: Stochastic optimization of energy hub operation with consideration of thermal energy market and demand response. Energy Convers. Manag. (2017). https://doi.org/10.1016/j.enconman.2017.04.074
23. Abou El-Ela, A.A.; El-Sehiemy, R.A.; Shaheen, A.M. et al: Enhanced coyote optimizer-based cascaded load frequency controllers in multi-area power systems with renewable. Neural Comput Applic. **33**, 8459–8477 (2021). https://doi.org/10.1007/s00521-020-05599-8
24. Zaky, A.A.; Ibrahim, M.N.; Rezk, H.; Christopoulos, E.; El Sehiemy, R.A.; Hristoforou, E.; Kladas, A.; Sergeant, P.; Falaras, P.: Energy efficiency improvement of water pumping system using synchronous reluctance motor fed by perovskite solar cells. Int. J. Energy Res. (2020). https://doi.org/10.1002/er.5788
25. Chan, D.S.H.; Phillips, J.R.; Phang, J.C.H.: A comparative study of extraction methods for solar cell model parameters. Solid. State. Electron. **29**, 329–337 (1986)
26. Jain, A.; Kapoor, A.: Exact analytical solutions of the parameters of real solar cells using Lambert W-function. Sol. Energy Mater. Sol. Cells. **81**, 269–277 (2004)
27. Saleem, H.; Karmalkar, S.: An analytical method to extract the physical parameters of a solar cell from four points on the illuminated *J–V* curve. IEEE Electron Device Lett. **30**, 349–352 (2009)
28. Agroui, K.; Pellegrino, M.; Giovanni, F.: Analysis techniques for photovoltaic modules based on amorphous solar cells. Arab. J. Sci. Eng. **42**, 375–381 (2017). https://doi.org/10.1007/s13369-016-2050-5
29. AlRashidi, M.R.; AlHajri, M.F.; El-Naggar, K.M.; Al-Othman, A.K.: A new estimation approach for determining the I–V characteristics of solar cells. Sol. Energy. **85**, 1543–1550 (2011)
30. El-Naggar, K.M.; AlRashidi, M.R.; AlHajri, M.F.; Al-Othman, A.K.: Simulated annealing algorithm for photovoltaic parameters identification. Sol. Energy. **86**, 266–274 (2012)
31. Jordehi, A.R.: Parameter estimation of solar photovoltaic (PV) cells: a review. Renew. Sustain. Energy Rev. **61**, 354–371 (2016)
32. Easwarakhanthan, T.; Bottin, J.; Bouhouch, I.; Boutrit, C.: Nonlinear minimization algorithm for determining the solar cell parameters with microcomputers. Int. J. Sol. Energy. **4**, 1–12 (1986). https://doi.org/10.1080/01425918608909835

33. Allam, D.; Yousri, D.A.; Eteiba, M.B.: Parameters extraction of the three diode model for the multi-crystalline solar cell/module using Moth-Flame Optimization Algorithm. Energy Convers. Manag. **123**, 535–548 (2016)
34. Awadallah, M.A.: Variations of the bacterial foraging algorithm for the extraction of PV module parameters from nameplate data. Energy Convers. Manag. **113**, 312–320 (2016)
35. Chen, X.; Yu, K.; Du, W.; Zhao, W.; Liu, G.: Parameters identification of solar cell models using generalized oppositional teaching learning based optimization. Energy (2016). https://doi.org/10.1016/j.energy.2016.01.052
36. Muhsen, D.H.; Ghazali, A.B.; Khatib, T.; Abed, I.A.: Extraction of photovoltaic module model's parameters using an improved hybrid differential evolution/electromagnetism-like algorithm. Sol. Energy. **119**, 286–297 (2015)
37. Muhsen, D.H.; Ghazali, A.B.; Khatib, T.; Abed, I.A.: Parameters extraction of double diode photovoltaic module's model based on hybrid evolutionary algorithm. Energy Convers. Manag. **105**, 552–561 (2015)
38. Alam, D.F.; Yousri, D.A.; Eteiba, M.B.: Flower pollination algorithm based solar PV parameter estimation. Energy Convers. Manag. **101**, 410–422 (2015)
39. Yuan, X.; Xiang, Y.; He, Y.: Parameter extraction of solar cell models using mutative-scale parallel chaos optimization algorithm. Sol. Energy. **108**, 238–251 (2014)
40. Oliva, D.; Cuevas, E.; Pajares, G.: Parameter identification of solar cells using artificial bee colony optimization. Energy (2014). https://doi.org/10.1016/j.energy.2014.05.011
41. Askarzadeh, A.; Rezazadeh, A.: Artificial bee swarm optimization algorithm for parameters identification of solar cell models. Appl. Energy. **102**, 943–949 (2013)
42. Askarzadeh, A.; Rezazadeh, A.: Parameter identification for solar cell models using harmony search-based algorithms. Sol. Energy. (2012). https://doi.org/10.1016/j.solener.2012.08.018
43. Ismail, M.S.; Moghavvemi, M.; Mahlia, T.M.I.: Characterization of PV panel and global optimization of its model parameters using genetic algorithm. Energy Convers. Manag. **73**, 10–25 (2013)
44. Askarzadeh, A.; dos Santos Coelho, L.: Determination of photovoltaic modules parameters at different operating conditions using a novel bird mating optimizer approach. Energy Convers. Manag. **89**, 608–614 (2015)
45. Qais, M.H.; Hasanien, H.M.; Alghuwainem, S.; Nouh, A.S.: Coyote optimization algorithm for parameters extraction of three-diode photovoltaic models of photovoltaic modules. Energy (2019). https://doi.org/10.1016/j.energy.2019.116001
46. Zaky, A.A.; Sehiemy, R.A.E.; Rashwan, Y.I.; Elhossieni, M.A.; Gkini, K.; Kladas, A.; Falaras, P.: Optimal performance emulation of PSCs using the elephant herd algorithm associated with experimental validation. ECS J. Solid State Sci. Technol. (2019). https://doi.org/10.1149/2.0271912jss
47. Bayoumi, A.S.; El-sehiemy, R.A.; Mahmoud, K.; Lehtonen, M.; Darwish, M.M.F.: Assessment of an Improved Three-Diode against Modified Two-Diode Patterns of MCS Solar Cells Associated with Soft Parameter Estimation Paradigms (2021)
48. Chen, H.; Jiao, S.; Heidari, A.A.; Wang, M.; Chen, X.; Zhao, X.: An opposition-based sine cosine approach with local search for parameter estimation of photovoltaic models. Energy Convers. Manag. **195**, 927–942 (2019)
49. Abbassi, R.; Abbassi, A.; Asghar, A.; Mirjalili, S.: An efficient salp swarm-inspired algorithm for parameters identification of photovoltaic cell models. Energy Convers. Manag. **179**, 362–372 (2019). https://doi.org/10.1016/j.enconman.2018.10.069
50. Khanna, V.; Das, B.K.; Bisht, D.; Singh, P.K.: others: A three diode model for industrial solar cells and estimation of solar cell parameters using PSO algorithm. Renew. Energy. **78**, 105–113 (2015)
51. Robandi, I., et al.: Photovoltaic parameter estimation using grey wolf optimization. In: 2017 3rd International Conference on Control, Automation and Robotics (ICCAR), pp. 593–597 (2017)
52. El-Sehiemy, R.A.; Shaheen, A.M.; Ginidi, A.; Ghoneim, S.S.M.: A forensic-based investigation algorithm for parameter extraction of solar cell models. IEEE Access. (2020). https://doi.org/10.1109/ACCESS.2020.3046536
53. Faramarzi, A.; Heidarinejad, M.; Mirjalili, S.; Gandomi, A.H.: Marine predators algorithm: A nature-inspired metaheuristic. Expert Syst. Appl. **152**, 113377 (2020)
54. Wolf, M.; Noel, G.T.; Stirn, R.J.: Investigation of the double exponential in the current–voltage characteristics of silicon solar cells. IEEE Trans. Electron Devices. **24**, 419–428 (1977)
55. Joshi, D.P.; Sharma, K.: Effects of grain boundaries on the performance of polycrystalline silicon solar cells. Ind. J Pure Appl. Phys. **50**(9), 661–669 (2012)
56. Fossum, J.G.; Lindholm, F.A.: Theory of grain-boundary and intragrain recombination currents in polysilicon pn-junction solar cells. IEEE Trans. Electron Devices. **27**, 692–700 (1980)
57. Koohi-Kamali, S.; Rahim, N.A.; Mokhlis, H.; Tyagi, V.V.: Photovoltaic electricity generator dynamic modeling methods for smart grid applications: a review. Renew. Sustain. Energy Rev. **57**, 131–172 (2016)